Diagnostic Systems in the Muon g-2 Experiment at Fermilab

Matteo Sorbara
on Behalf of the Muon g-2 Collaboration

University and INFN Roma "Tor Vergata"

International Conference on Frontier in Diagnostic Tecnologies
Frascati, 21-23 October 2024

Sections

Spin Precession in a Magnetic Field

A particle's spin in a magnetic field experience a torque and a precession motion proportional to it's magnetic moment, defined as

$$\vec{\mu} = g\frac{e}{2m}\vec{S}$$

The spin precession frequency is given by:

$$\omega_s = g\frac{e}{2m}B$$

- Dirac equation predicts naturally $g = 2$ for a spin $\frac{1}{2}$ elementary particle
- Define the anomaly as $a_\mu := \frac{g-2}{2}$
- Radiative corrections give a positive contribution. Schwinger: $a_\mu \sim \frac{\alpha}{2\pi} \approx 0.00116$ (at first order)

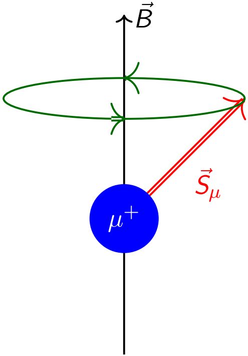

Standard Model Prediction of a_μ

$a_\mu = 0$

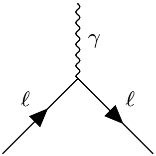

Dirac

Standard Model Prediction of a_μ

$$a_\mu = 0 + a_\mu^{QED}$$

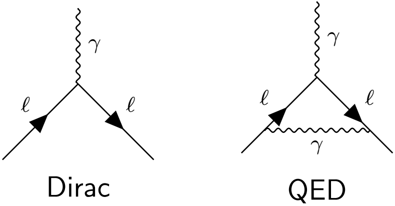

- Highest and most precise contribution to a_μ
- Computed perturbatively

$$a_\mu^{QED} = \sum_{n\geq 1} c^{(2n)} \left(\frac{\alpha}{\pi}\right)^n$$

Standard Model Prediction of a_μ

$$a_\mu = 0 + a_\mu^{QED} + a_\mu^{W}$$

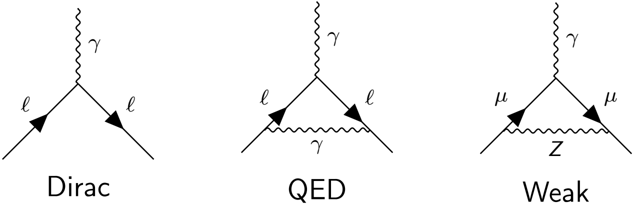

- Contribution due to the $Z,\ W,\ H$ exchange
- Computed at 2 loops level
- Well known and with small uncertainty

Standard Model Prediction of a_μ

$$a_\mu = 0 + a_\mu^{QED} + a_\mu^{W} + a_\mu^{HLbL}$$

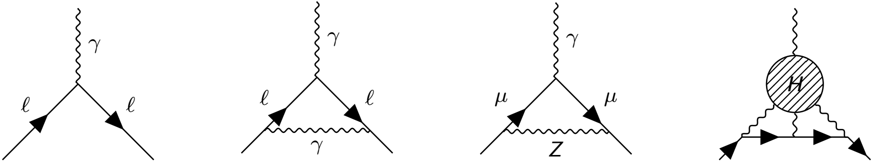

Dirac QED Weak Hadronic LbL

- Second dominant uncertainty source
- At low energies:
  - Data driven
  - Lattice QCD
- Perturbative QCD for c-quark loops

Standard Model Prediction of a_μ

$$a_\mu = 0 + a_\mu^{QED} + a_\mu^{W} + a_\mu^{HLbL} + a_\mu^{HVP}$$

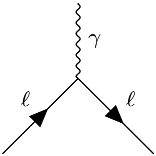

Dirac

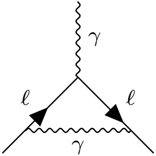

QED

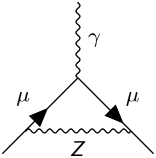

Weak

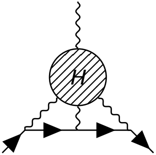

Hadronic LbL

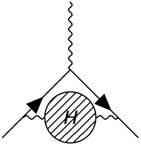

Hadronic Vacuum Polarization

- Dispersive (data driven):

$$a_\mu^{HVP,LO} = \frac{1}{4\pi^3} \int_{m_\pi^2}^{\infty} ds\ K(s)\ \sigma^0_{e^+e^- \to had}$$

- Lattice QCD calculation shows a discrepancy with the dispersive approach

How to measure a_μ

The measurement is based on the anomalous spin precession frequency:

$$\vec{\omega}_a = \vec{\omega}_{spin} - \vec{\omega}_{cyclotron} = a_\mu \frac{e\vec{B}}{mc}$$

- $a_\mu = 0$ spin and momentum precess at the same rate

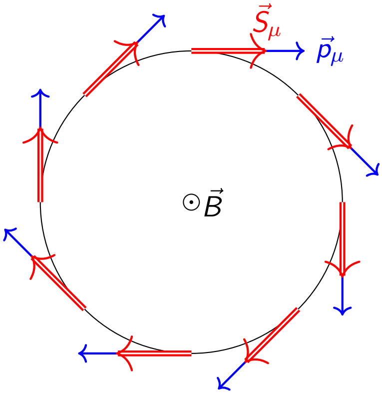

How to measure a_μ

The measurement is based on the anomalous spin precession frequency:

$$\vec{\omega}_a = \vec{\omega}_{spin} - \vec{\omega}_{cyclotron} = a_\mu \frac{e\vec{B}}{mc}$$

- $a_\mu = 0$ spin and momentum precess at the same rate
- $a_\mu > 0$ the spin has a precession motion around the momentum direction

a_μ can be extracted from a polarized muon beam by measuring ω_a and B:

$$a_\mu = \frac{\omega_a}{B} \cdot \frac{mc}{e}$$

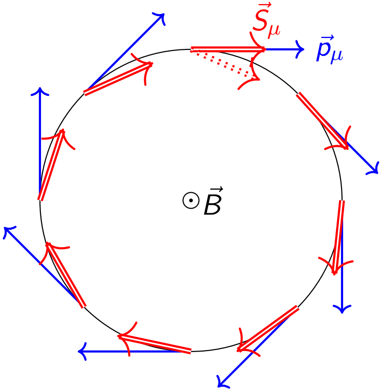

How to measure a_μ (for real)

$$a_\mu = \frac{\omega_a}{\tilde{\omega}'_p(T)} \underbrace{\frac{\mu'_p(T)}{\mu_e} \frac{m_\mu}{m_e} \frac{g_e}{2}}_{\text{External}}$$

Magnetic field is expressed in term of the shielded proton precession frequency (ω'_p). External factors are known to very high precision (22 ppb uncertainty).

We extract the ratio:

$$R'_\mu = \frac{\omega_a}{\tilde{\omega}'_p(T)} = \frac{f_{clock} \cdot \omega_a^{meas} \cdot \overbrace{(1 + C_e + C_p + C_{dd} + C_{ml} + C_{pa})}^{\text{Beam Dynamics}}}{f_{calib} \cdot \langle \omega'_p(x,y,\phi) \cdot M(x,y,\phi) \rangle \cdot \underbrace{(1 + B_k + B_q)}_{\text{Transient Fields}}}$$

- ω_a^{meas} is the the measured precession frequency
- $\tilde{\omega}'_p(T)$ is the the magnetic field magnitude averaged around the ring
- $M(x,y,\phi)$ is the beam distribution along the ring

Muons production

- LINAC produces 400 MeV proton beam
- Protons accelerated to 8 GeV in Booster

Muons production

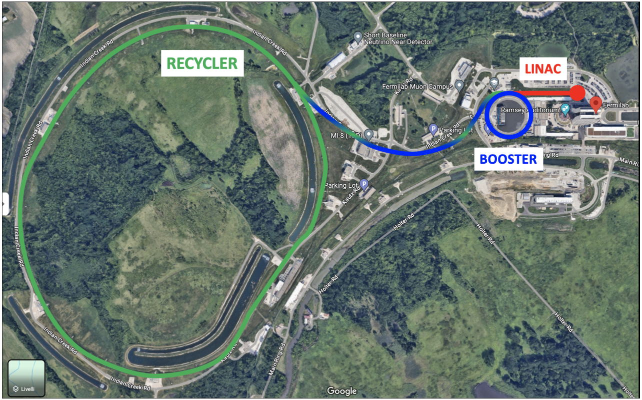

- Rebunching in the Recycler Ring
- Proton bunches sent to the Target Station

Muons production

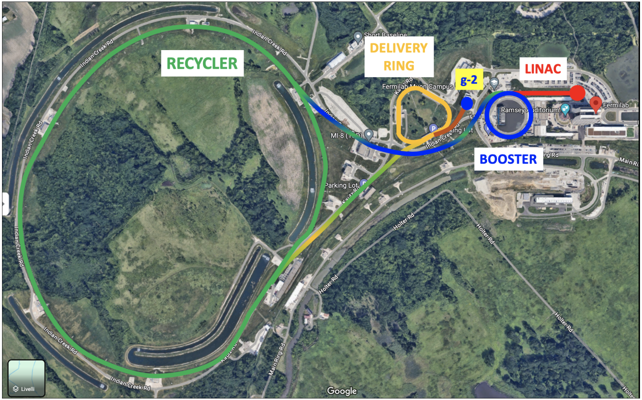

- Protons are smashed on a Ni/Cr target to produce π^+
- p, μ^+, π^+ are selected in momentum and sent into the delivery ring
- π^+ decay, p are separated, polarized muons are sent to the g-2 storage ring

One Ring to Store Them All

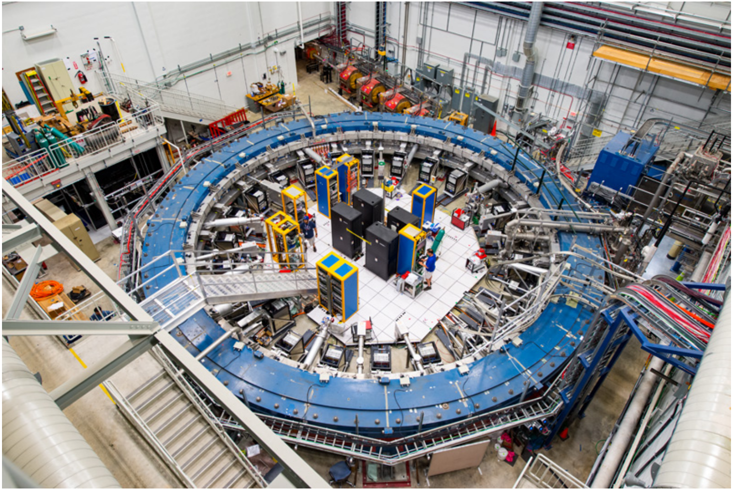

One Ring To Store Them All

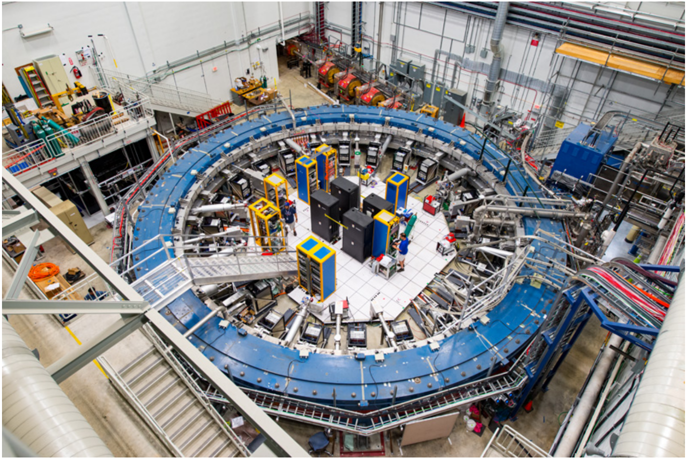

One Ring To Store Them All

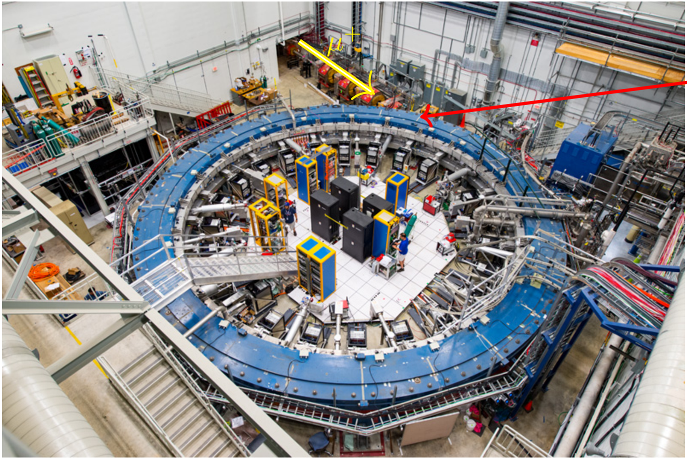

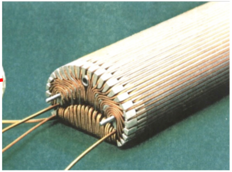

Inflector

One Ring To Store Them All

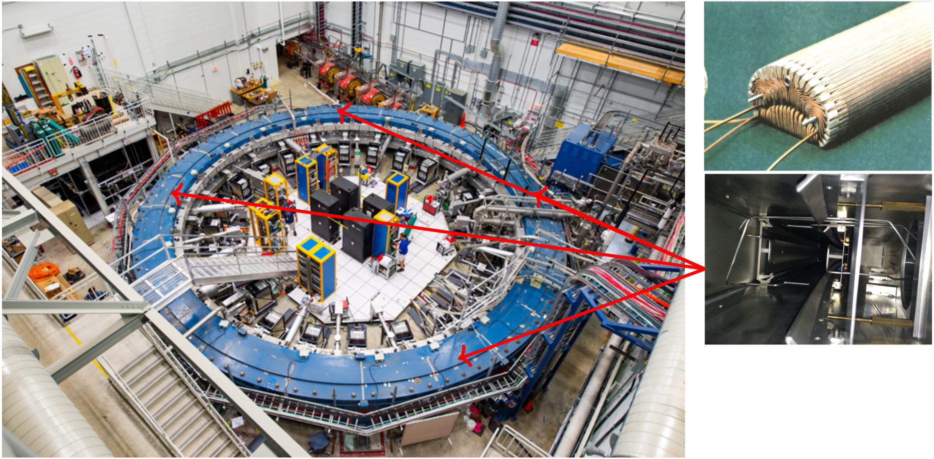

Quadrupoles

One Ring To Store Them All

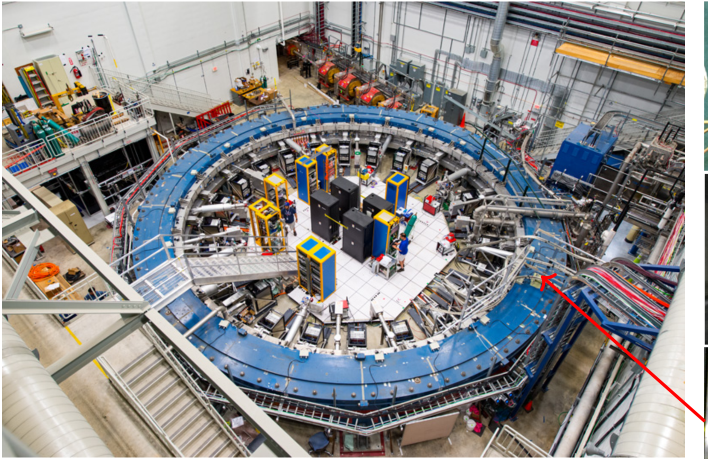

Kickers

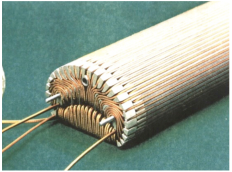

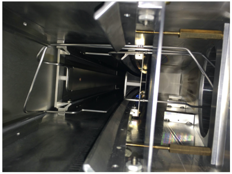

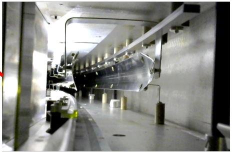

How to measure the spin precession frequency

The muon polarization is measured using the parity-violating decay

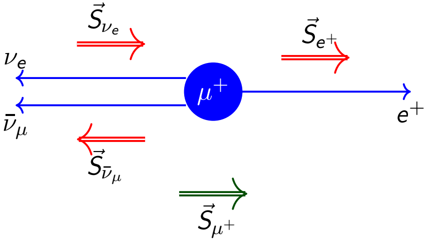

High momentum e^+ are emitted preferentially in the muon's spin direction

Count the number of high energy positrons in a given direction as a function of time to extract the precession frequency

Detect decay positrons

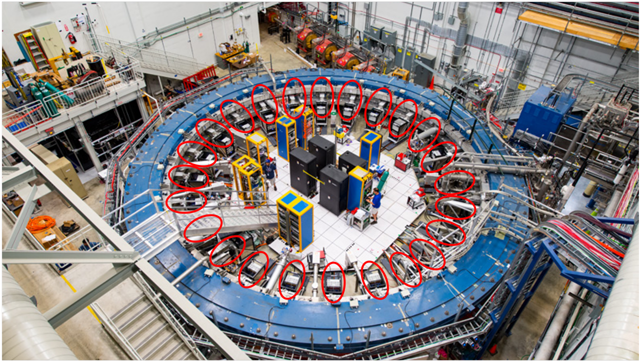

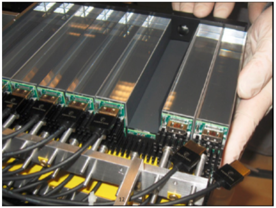

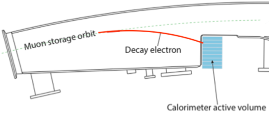

- 24 PbF2 calorimeters along the inner circumference (out of vacuum)
- Čerenkov light is read by large area SiPM
- Gain is monitored at a 10^{-4} level of stability by state of the art Laser Calibration System

The anomalous precession frequency

The time distribution of the high energy positrons shows the muons exponential decay modulated by the anomalous precession frequency. The distribution is fitted to extract ω_a:

$$N(t) = N_0 * e^{-\frac{t}{\tau_\mu}} \cdot [1 - A\cos(\omega_a \cdot t + \varphi)] + \mathcal{C}$$

Corrections to the equations include:

- Beam Dynamic terms to account for beam oscillations that distort the modulation signal
- Muon Losses that distort the exponential shape of the distribution

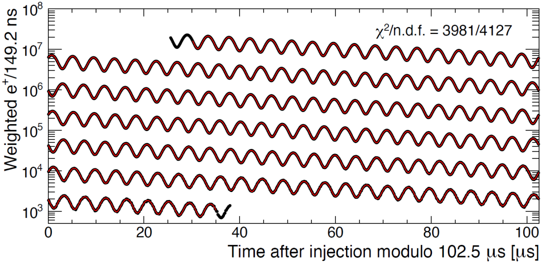

Weighted Magnetic Field

- A trolley is equipped to measure the magnetic field inside the storage region
- Dedicated runs every 2/3 days when beam is off
- A field map in the storage region is interpolated in time to get the field during data taking period (more later)
- The field map is averaged over the azimuth and weighted with the muons distribution

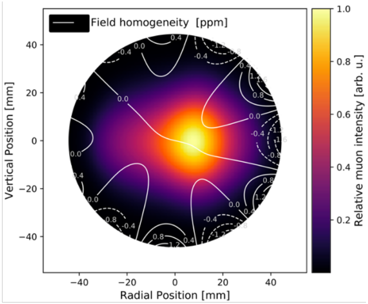

Results (Run 1)

At this point the muon anomaly can be computed:

$$a_\mu = \frac{\omega_a}{\tilde{\omega}'_p(T)} \frac{\mu'_p(T)}{\mu_e} \frac{m_\mu}{m_e} \frac{g_e}{2}$$

First result published on April 2021:

- Based on 5% of the data collected
- Confirmed BNL experiment result (20 years before)
- Increased the discrepancy with the Theory Initiative White Paper to 4.2σ

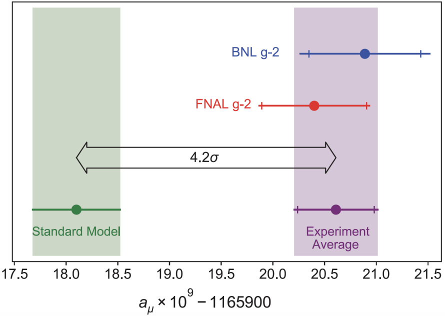

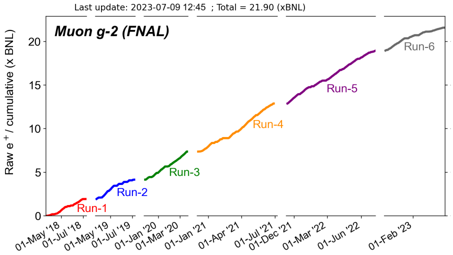

Results (Run 2 and Run 3)

New result released on the 10th of August 2023

- Result paper: **Phys.Rev.Lett. 131 (2023) 16, 161802**; Analysis Details: **Phys.Rev.D 110 (2024) 3, 032009**
- In excellent agreement with both BNL and Run 1 result
- Reduced by a factor 2.2 statistical and systematic uncertainty

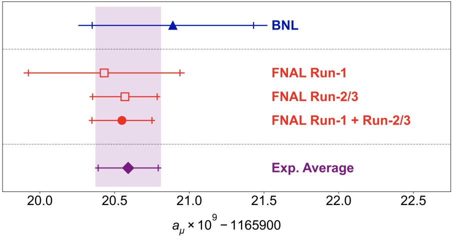

$$a_\mu^{Run2-3} = 116\,592\,057(25) \times 10^{-11} \quad [0.21 \text{ ppm}]$$
$$a_\mu^{Run1-2-3} = 116\,592\,055(24) \times 10^{-11} \quad [0.20 \text{ ppm}]$$
$$a_\mu^{ExpAvg} = 116\,592\,059(22) \times 10^{-11} \quad [0.19 \text{ ppm}]$$

Beam injection monitors

- T0 detector
- Made of a slab of plastic scintillator read by two PMTs
- Positioned at the end of the beamline out of vacuum
- Provides the trigger at the beam injection
- The integral of the T0 counts also provide the number of injected muons

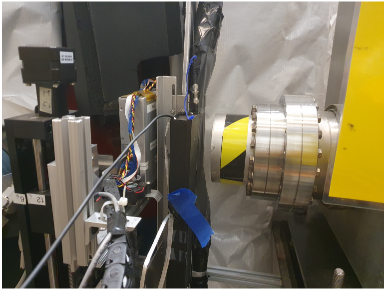

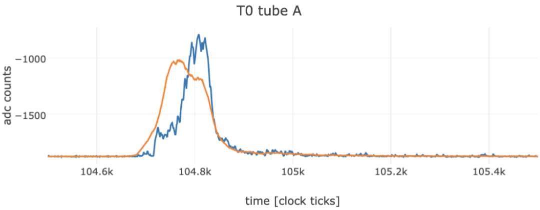

Beam injection monitors

- Inflector Beam Monitoring Station (IBMS)
- Two detectors placed along the beamline
- Set of scintillating fibers in a grid pattern
- Provides the beam profile at the entrance of the storage ring before the inflector
- Used for beam monitoring and tuning

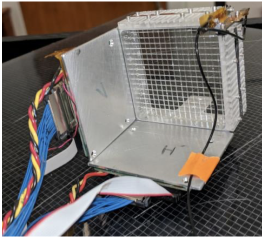

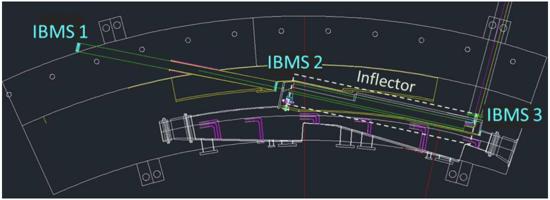

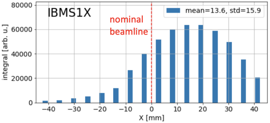

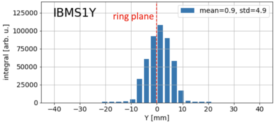

Beam Distribution

- Beam reconstruction is crucial for the analysis
- Two tracker stations at 180° and 270° azimuth angle
- 8 modules with 32 straw tubes in stereo pattern (give x and y)
- Provides a non-destructive reconstruction of the beam position over time

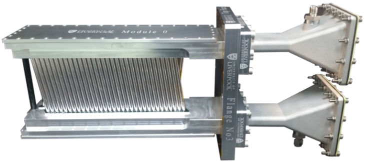

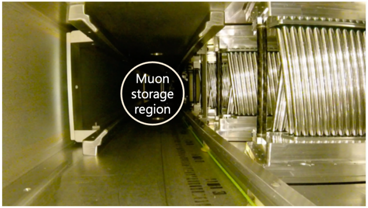

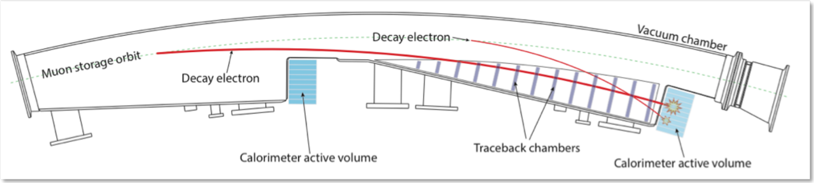

Beam Distribution

- Track is reconstructed by fitting the hit points on each straw
- The fitted track is extrapolated backwards to reconstruct the muon decay vertex point
- The track curvature provides a momentum measurement of the particle
- Using the particle momentum and the energy deposit in the calorimeter is possible to keep track of the muons not stored

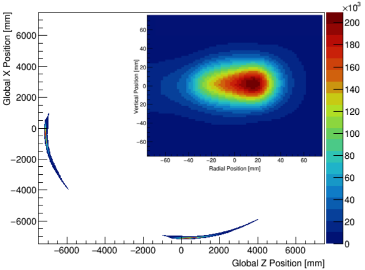

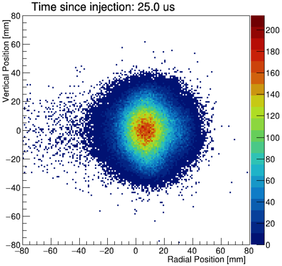

Magnetic field

- Magnetic field monitoring is based on Nuclear Magnetic Resonance techniques
- Absolute field is measured from the precession frequency of the proton in the NMR probes
- 378 probes continuously measure the field around the vacuum chamber
- A trolley equipped with 17 probes is used to track the magnetic field in the muon storage region (edicated runs every 2/3 days)

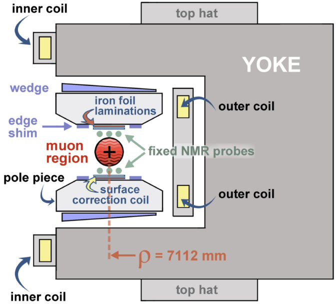

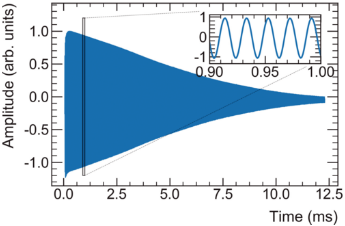

Calorimeter Gain Corrections

- At beam injection a large flux of particles hit the calorimeters
- SiPMs gain drops due to the high number of hits
- $\mathcal{O}(10\ \mu s)$ recovery time
- Laser system measures the calorimeter response as a function of time
- Positron energy is corrected:

$$E_{true} = E_{SiPM} \cdot \frac{1}{1 - \alpha e^{-t/\tau}}$$

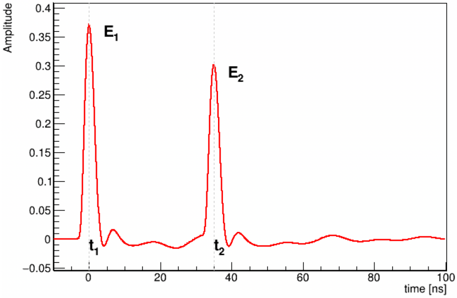

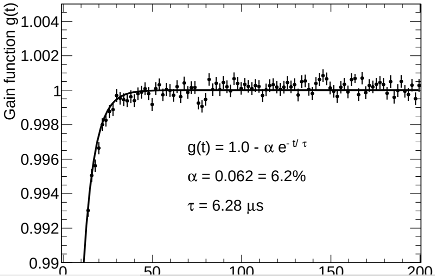

Laser Calibration System

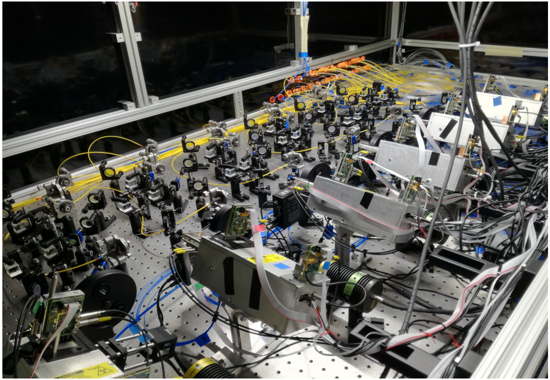

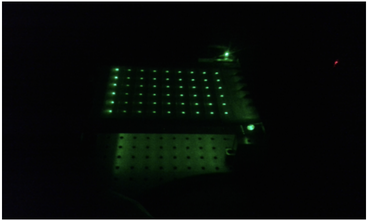

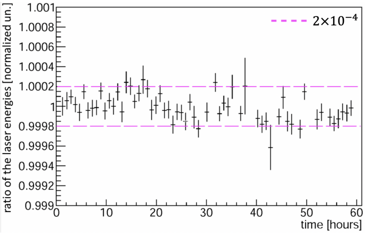

- The calibration system provides a laser pulse in each of the 1296 crystals to keep track of any gain variation
- The system has two monitors to keep the laser pulses stable at $\mathcal{O}(10^{-4})$ level

Conclusions

- High precision physics can be reached only with a precise knowledge of all the experiment subsystems
- Muon g-2 uses these diagnostic systems to track and reduce systematics associated with the instrumentation
- Reached the goal of 70 ppb of systematic uncertainties from the TDR
- Achieved precision of 0.19 ppm on the combined a_μ measurement
- Full statistics is under analysis to reach the goal of 0.14 ppm stated at the beginning of the experiment

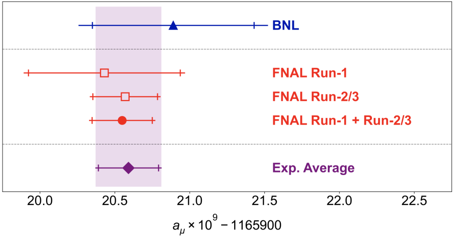

BACKUP

Run 2-3 improvements

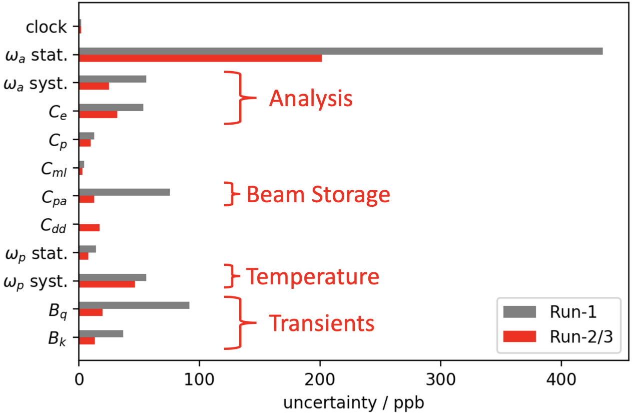

Total Uncertainty:

$$\sigma^{Run1} = 434^{\text{Stat}} + 157^{\text{Syst}} \text{ ppb}$$
$$\sigma^{Run2-3} = 201^{\text{Stat}} + 70^{\text{Syst}} \text{ ppb}$$

Theory Comparison

- Fermilab result alone yelds to a $> 5\sigma$ discrepancy with the 2020 Theory Initiative calculation

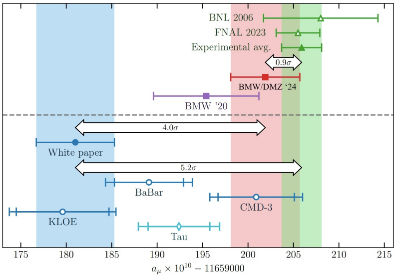

BMW/DMZ24 Collaborations arXiv: 2407.10913

Theory Comparison

- Fermilab result alone yelds to a $> 5\sigma$ discrepancy with the 2020 Theory Initiative calculation
- HVP value from lattice calculations reduces the discrepancy with the experimental value

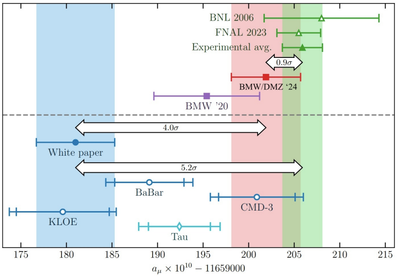

BMW/DMZ24 Collaborations arXiv: 2407.10913

Theory Comparison

- Fermilab result alone yelds to a $> 5\sigma$ discrepancy with the 2020 Theory Initiative calculation
- HVP value from lattice calculations reduces the discrepancy with the experimental value
- Recent results on $e^+e^- \to \pi^+\pi^-$ cross section from CMD-3 (below 1 GeV) further reduces the discrepancy
- Many efforts on the theory side to resolve theoretical ambiguities

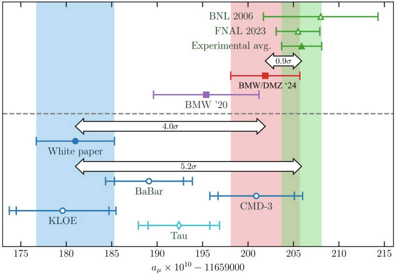

BMW/DMZ24 Collaborations arXiv: 2407.10913

Hadronic Vacuum Polarization

Dispersion integral from the optical theorem:

$$a_\mu^{HVP,LO} = \frac{\alpha^2}{3\pi^2} \int_{m_\pi^2}^{+\infty} \frac{K(s)}{s} R(s) ds$$

with

$$R(s) = \frac{\sigma^0(e^+e^- \to \text{hadrons})}{\sigma_{pt}(e^+e^- \to \mu^+\mu^-)}$$

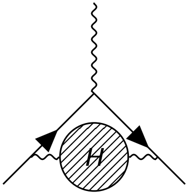

	Value (10^{-11})	Uncertainty (10^{-11})
QED	116 584 718.931	0.104
Weak	153.6	1.0
HVP	6845	40
HLbL	92	18
Total	116 591 810	43
HVP_L	6989	55

$a_\mu^{HVP,LO}$ and running of α

Hadronic contribution to the running of the QED coupling constant at M_Z

$$\Delta\alpha_{had}(M_Z^2) = \frac{M_Z^2}{4\alpha\pi^2}\int_{m_\pi^2}^{\infty}\frac{ds}{M_Z^2 - s}\,\sigma^0(e^+e^- \to hadrons)$$

while

$$a_\mu^{HVP,LO} = \frac{1}{4\pi^3}\int_{m_\pi^2}^{\infty} ds\ K(s)\ \sigma^0(e^+e^- \to hadrons)$$

Missing contributions in the hadronic cross section:

- $\sqrt{s} \gtrsim 1$ GeV excluded by constraints from the global EW fit at 95% C.L.
- $\sqrt{s} \lesssim 1$ GeV one order of magnitude larger than the experimental uncertainty

- A. Keshavarzi, W. J. Marciano, M. Passera, A. Sirlin - Muon $g-2$ and $\Delta\alpha$ connection - Phys. Rev. D 102, 033002 (2020)

Quis custodiet ipsos custodes?

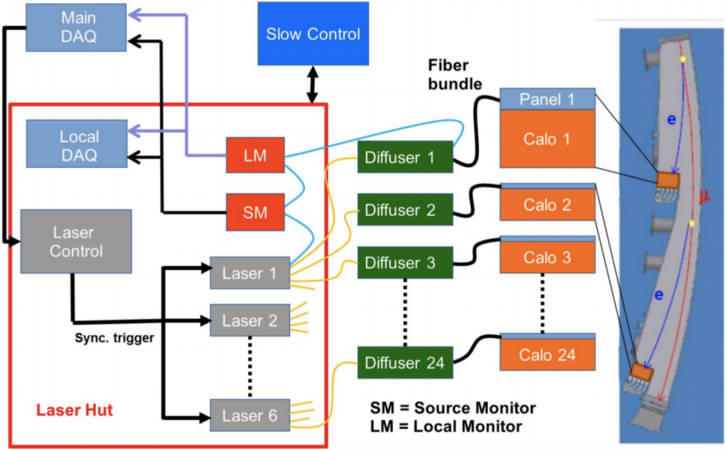

Run 2-3 improvements

After Run 1 many efforts were done to improve the uncertainties:

- Statistics
  - Factor 4.7 in the number of analyzed positrons (weighted, $E > 1$ GeV, $t > 30\ \mu$s)
  - Statistical uncertainty decreased from 434 ppb (Run 1) to 201 ppb (Run 2-3)

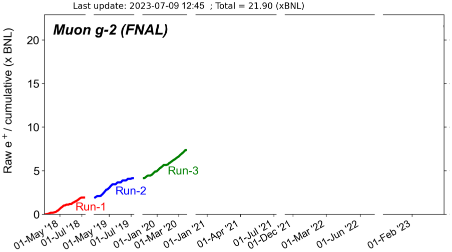

After Run 1 many efforts were done to improve the uncertainties:

- Statistics
- Beam Storage - Quadrupoles
  - Damaged resistors in Run 1 caused beam motion during the fill; re-designed for Run 2 to reduce beam motion
  - Reduced uncertainty on C_{pa} from 75 ppb to 13 ppb

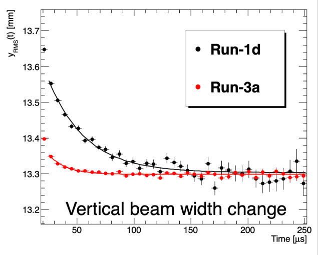

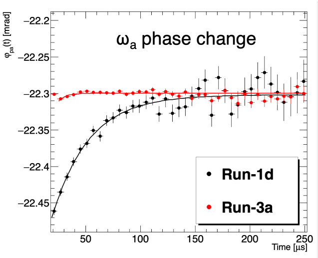

Run 2-3 improvements

After Run 1 many efforts were done to improve the uncertainties:

- Statistics
- Beam Storage - Quadrupoles
- Beam Storage - Kickers
  - Kickers strength improved to design value at the end of Run 3
  - Beam more centered, reduced oscillations

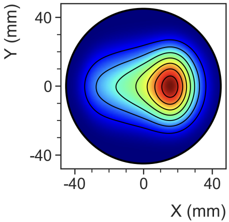

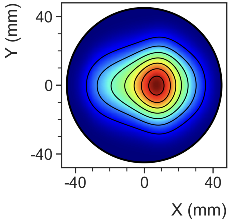

Run 2-3 improvements

After Run 1 many efforts were done to improve the uncertainties:

- Statistics
- Beam Storage - Quadrupoles
- Beam Storage - Kickers
- Temperature stability
  - Thermal insulation added to the ring between Run 1 and Run 2 to improve thermal stability of the magnet
  - A/C hall cooling after Run 2 further improved the stability
  - Reduced magnetic field and SiPM gain variations due to temperature

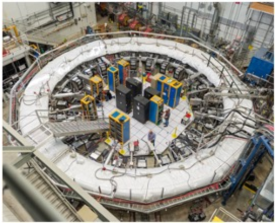

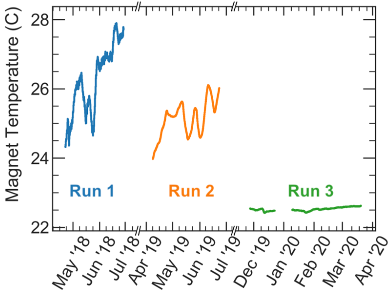

Run 2-3 improvements

After Run 1 many efforts were done to improve the uncertainties:

- Statistics
- Beam Storage - Quadrupoles
- Beam Storage - Kickers
- Temperature stability
- Field Transient Measurement
  - Quadrupoles transient field B_q measured all around the ring (only 2 locations in Run 1)
  - Improved Kicker transient field measurement with fiber magnetometer

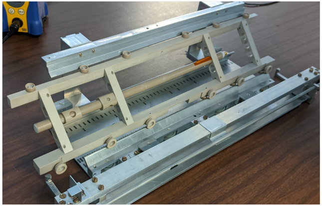

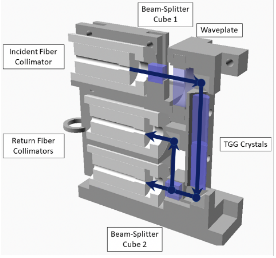

Run 2-3 improvements

After Run 1 many efforts were done to improve the uncertainties:

- Statistics
- Beam Storage - Quadrupoles
- Beam Storage - Kickers
- Temperature stability
- Field Transient Measurement
- Analysis Technique Improvements
  - New positron reconstruction algorithms
  - Improved Pile-Up subtraction technique

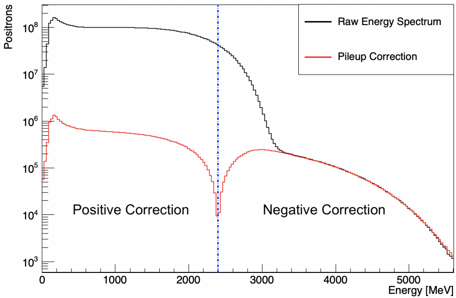

The ω_a equation

Including beam motion and relativistic effects the anomalous precession frequency becomes:

$$\vec{\omega}_a = -\frac{e}{mc}\left[a_\mu \vec{B} - \left(a_\mu - \frac{1}{\gamma^2 - 1}\right)\vec{\beta}\times\vec{E} - a_\mu \frac{\gamma}{\gamma + 1}\left(\vec{\beta}\cdot\vec{B}\right)\vec{\beta}\right]$$

- The electric field term is due to the focussing electrostatic quadrupoles; for $\gamma = 29.3$ it becomes negligible;
- The magnetic field term is due to the beam vertical oscillation;
- Precisely measure ω_a and the B-field to measure a_μ.

Typical Beam Frequencies

$$n = -\frac{R_0}{vB_0}\frac{\partial E_y}{\partial y}$$

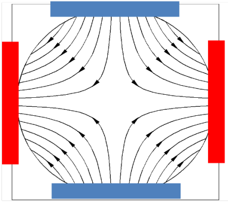

Name	Symbol	Expression	Frequency [MHz]
Cyclotron	f_c	$\frac{v}{2*\pi*R_0}$	6.71
Horizontal Betatron	f_x	$f_c\sqrt{1-n}$	6.33
Vertical Betatron	f_y	$f_c\sqrt{n}$	2.20
Coherent Betatron	f_{CBO}	$f_c - f_x$	0.37
Vertical Waist	f_{VW}	$f_c - 2f_y$	2.30
Anomalous Precession	f_a	$a_\mu eB/m$	0.2292

Detectors Resolutions

Calorimeter:

- Energy: $4.6\%/\sqrt{E}$
- Time: 20 ps on a single crystal
- Space: $\mathcal{O}(1\text{ mm})$

Tracker:

- Space: 110 μm
- Time: 1 ns
- Efficiency: 99% (97% at the edge of the straw)